Solar Energy 307 (2026) 114364

Contents lists available at ScienceDirect

Solar Energy

journal homepage: www.elsevier.com/locate/solener

A parametric evaluation of rooftop photovoltaic utilization and yield density considering urban morphology effects

Fatma Fathy [a,b,1,*], Rabee Shamass [a,2], Xiangming Zhou [a,3]

[a] Brunel University of London, Civil and Environmental Engineering Department, United Kingdom
[b] Ain Shams University, Faculty of Engineering, Architecture Department, Egypt

ARTICLE INFO

Keywords:
Renewable Energy
PV Utilization
Urban Morphology
Building Performance Simulation
Regression Analysis

ABSTRACT

Urban morphology plays a critical role in shaping the energy utilization potential of rooftop photovoltaic (PV) systems, with key factors including building height, available roof area, as well as obstruction angles and orientation influencing shading patterns and solar exposure. Previous research highlighted the impact of building and urban forms on enhancing solar energy utilization and decreasing energy demands. However, the development of a simple design model that captures the relationship between key design parameters and their impact on PV Utilization potential and Yield Density requires further large-scale investigation. This study aims to develop design-oriented regression models that enable practitioners to reliably estimate PV technical potential in the early stages of the design process. A comprehensive parametric analysis with around 1,000 simulation runs were conducted to evaluate and predict rooftop PV energy performance, emphasizing the influence of building and urban design parameters. Correlation analysis and regression models are developed to interpret the parametric relations and utilization potential of PV on building's rooftop in Cairo, Egypt. Results indicate that roof-to-total floor area (RTFA %) and sunhours % are the most significant predictors of PV Utilization. These variables interact such that the sensitivity of PV Utilization in response to sunhours variations is doubled with every increase in RTFA %. In contrast, sunhours % and South obstruction angle are found to be the effective predictors of PV Yield Density. This study provides valuable insights for informed decision making, enabling the design of urban environments that maximize solar energy utilization and support sustainable development.

1. Introduction

Buildings account for around 30 % of global energy consumption and are responsible for nearly 26 % of energy-related emissions worldwide [1]. The need to generate energy from renewable resources is urgingly rising to fulfill the global requirements, long-term sustainability and energy security goals. Efforts are focused on making renewable energy contribute two-thirds of the total energy supply by 2050 [2]. It is expected that transition to renewable energy in power generation will have the most significant reduction share of carbon dioxide (CO_2) emissions to achieve net-zero targets by 2050 under the 1.5°C climate pathway [3]. Solar energy is one of the most utilized sources of energy. Advances of technology such as Photovoltaic (PV) systems make it a reliable source of clean energy with improved power generation and decreased life cycle costs [4]. Global PV capacity has increased from 100 GW in 2012 to 942 GW in 2021, showing an increase of 842 % in this period [5]. In 2021, solar PV capacity in the Middle East and Africa increased by approximately 5.2 GW, representing a 3 % annual growth and bringing the regional total to 28 GW. However, despite the region's high solar irradiance, only a limited number of countries exceeded the 5 % threshold of electricity demand met by solar PV, where Egypt reached around 3 % [6].

Governments should provide specific incentives for using underutilized spaces like building rooftops for clean energy installations, avoiding the need for new land development. Additionally, simplifying permitting processes for small-scale projects, like residential solar panels, can remove administrative difficulties and encourage wider adoption [7]. In

* Corresponding author at: Brunel University of London, Civil and Environmental Engineering department, United Kingdom.
E-mail addresses: fatema.abdelaziz@brunel.ac.uk, fatma.fathy@eng.asu.edu.eg (F. Fathy), Rabee.Shamass@brunel.ac.uk (R. Shamass), Xiangming.Zhou@brunel.ac.uk (X. Zhou).
[1] https://orcid.org/0000-0001-8661-8407.
[2] https://orcid.org/0000-0002-7990-8227.
[3] https://orcid.org/0000-0001-7977-0718.

https://doi.org/10.1016/j.solener.2026.114364
Received 23 October 2025; Received in revised form 14 January 2026; Accepted 18 January 2026
Available online 24 January 2026

Egypt, the government has taken significant steps and introduced incentives to promote the use of renewable energy. These include tax exemptions for electricity production projects based on renewable sources aiming to increase the share of renewable energy to 42 % by 2030 [8].

Egypt is characterized by high solar radiation with an average solar radiation ranging from 2,000 to 3,200 kWh/m^2 annually. This high level of solar irradiance provides the country with considerable potential for harnessing renewable solar energy [9]. In 2024, solar energy from photovoltaic (PV) panels accounted for 32 % of the total renewable electricity generated, ranking second after hydropower (37%), while wind accounted for 28%, other solar technologies 2%, and biomass 1% [8]. However, rooftop PV represents a small fraction of national PV capacity due to both logistical and regulatory issues. It is only concentrated on pilot projects and a small number of residential installations. By 2021, only 125 small-scale systems of around 11 MW capacity were installed across 15 governorates, despite Egypt's broader renewable goals [6].

Rooftop PV systems offer opportunities for clean energy generation and carbon emission reductions within urban contexts. Nguyen et al. [10] estimated that around one third of the roof areas are available in cities, highlighting the potential of applying PV systems on rooftops. Their effectiveness in mitigating uprising environmental pressures was addressed in various studies [11–14]. Pan et al. [13] estimated that Guangzhou city has 391.7 km^2 of suitable rooftop area with PV energy potential ranging from 44.06 to 72.12 billion kWh annually and corresponding reductions in power sector carbon emissions ranging from 72.12 % to 100 %. Gomez-Exposito et al. [15] showed that more than 95 % of the cities in Spain possess rooftop PV potential exceeding their annual electricity demand. It was estimated that a maximum capacity of 234 GW installed on 1,134 km^2 of available rooftop area can be reached, excluding north-facing surfaces. This corresponded to 46 % of the total urban area and only 0.22 % of the Spanish national land area, capable of generating approximately 290 TWh of electricity annually. Hong et al. [16] estimated the suitable rooftop areas for installing PV panels in Seoul, South Korea, using Hillshade analysis. They found that suitable roof area in Gangnam district reached around 4,964 km^2 accounting for 66 % of the total area and a PV potential of around 1,130 GWh. Walch et al. [17] used machine learning, GIS and physical models to estimate PV potential of 9.6 million rooftops in Switzerland, showing that 55 % of roof areas were suitable for PV installation, which can account for around 40% of annual electricity demand. Alhammami et al. [18] showed that Khalifa and Zayed City in Abu Dhabi, UAE cover total areas of 23.39 km^2 and 49 km^2, respectively, with rooftops representing around 12.6 % of the total area. Based on rooftops utilization factors ranging from 0.25 to 0.45, they estimated annual energy potential at 116.3–211.7 GWh and 249–448.2 GWh, respectively. These studies estimated the PV energy generation based on the available solar potential on the macroscale of urban clusters and the city scale level.

Making the best use of underutilized areas like rooftops requires special attention to the building scale and the resultant factors that affect solar energy utilization potential. Fakhraian et al. [14] classified these factors based on four sub-potentials including physical, geographic (urban), technical and economic potential. The physical potential referred to the solar energy received based on climatic conditions. The technical potential represented the electricity production determined by technical characteristics like PV efficiency and PV performance. The economic potential encompassed cost-related and social constraints. Additionally, the geographic or urban potential involved factors like building layout and urban context which impact shadow patterns and solar irradiance [19,20]. These shadow patterns were found to significantly impact the performance of rooftop PV systems. Ren et al. [21] stated that reductions in PV energy generation reached up to 39.71% under high shadows from neighboring buildings. Xie et al. [22] investigated the impact of block typology and urban morphology on the energy consumption and solar energy potential, indicating a possible 12.25 % difference in energy use intensity (EUI) and 30.88% in solar energy generation intensity (SEGI). The primary parameters included shape factor which affected both EUI and SEGI. Tower blocks were found to have the best SEGI with the lowest net EUI, whereas the H and U-shaped blocks had the lowest EUI from other shape types. Other parameters like average block length and building density affected EUI, while the average height of the block and sky view factor influenced more solar energy generation. Wang et al. [23] also showed that there was a significant inter-building effect on both energy consumption and PV Utilization which varied greatly based on the climatic zone. Li et al. [24] investigated the impact of building shape layouts on PV Utilization, recommending U-shaped and courtyard blocks. The U-shaped layout achieved the highest energy generation at 143 kWh/m^2, while the courtyard shape had the highest installation area ratio of 0.68. Liu et al. [25] assessed 17 morphological indicators on PV potential using 300 building clusters as a sample of rural buildings in Nanjing, China, demonstrating that building height and floor area ratio are the most influential factors. These studies relied on complex building performance simulations (BPS), highlighting the need for direct and generalized methods to estimate or predict PV performance that can be easily applied by users.

Building Performance Simulation (BPS) and optimization are essential for assessing PV energy performance; however, due to the time-consuming nature and lack of skill of this computational approach, environmental assessments are often left to late stages of the design or even neglected [26]. Jiang et al. [27] highlighted challenges of adopting traditional BPS, particularly its dependence on detailed models and expert data input, which limits its scalability and early-stage adoption in design processes. To address this limitation, developing user-friendly predictive models is valuable in providing early results with quick feedback on PV Utilization potential with the least possible resources. Although previous research studies have examined the impact of geographic parameters on PV Utilization, there remains a gap in providing designers with simple, practical models that can be used in the early design phase to estimate rooftop PV technical potential.

This paper aims to address this gap by developing predictive models that directly estimate design performance in terms of solar potential, linking building and context parameters to rooftop PV Utilization and Yield Density potential. The goal is to estimate the percentage of a building's energy demand that can be met by rooftop PV system (PV Utilization). By evaluating both the capacity for PV energy generation and the total building energy use, this study seeks to estimate the percentage of PV Utilization for various building configurations. In addition, it calculates the PV Yield Density, defined as the annual energy generated per one meter square of PV panel. To achieve this, around 1,000 rooftop PV installations are simulated using Climate Studio tool, providing a wide range of design parameters by varying building length, width, height, and the orientation and angles of surrounding obstructions. Correlation analysis is then employed to identify key parameters influencing PV performance, while regression models are developed to predict PV Utilization and Yield Density as a function of building form and surrounding obstruction variables.

This paper is structured into three main sections. First, it outlines the proposed methodology, which includes a parametric simulation analysis of the case study and the development of regression models. Next, the results and discussion section presents the prediction performance of the developed regression models for PV Utilization and Yield Density. Finally, the conclusion highlights the impact of rooftop PV installations on energy reduction, emphasizes the critical role of building and urban configurations, and underscores the novelty of the proposed approach while suggesting directions for future research.

2. Methodology

Reliable predictions of rooftop PV energy generation are influenced by several variables, including climatic conditions, sun exposure hours and the available rooftop area for PV installations. This study investigates the hot climatic context of Cairo, Egypt having Latitude 30°N and Longitude 31°E using a generic office building as a case study

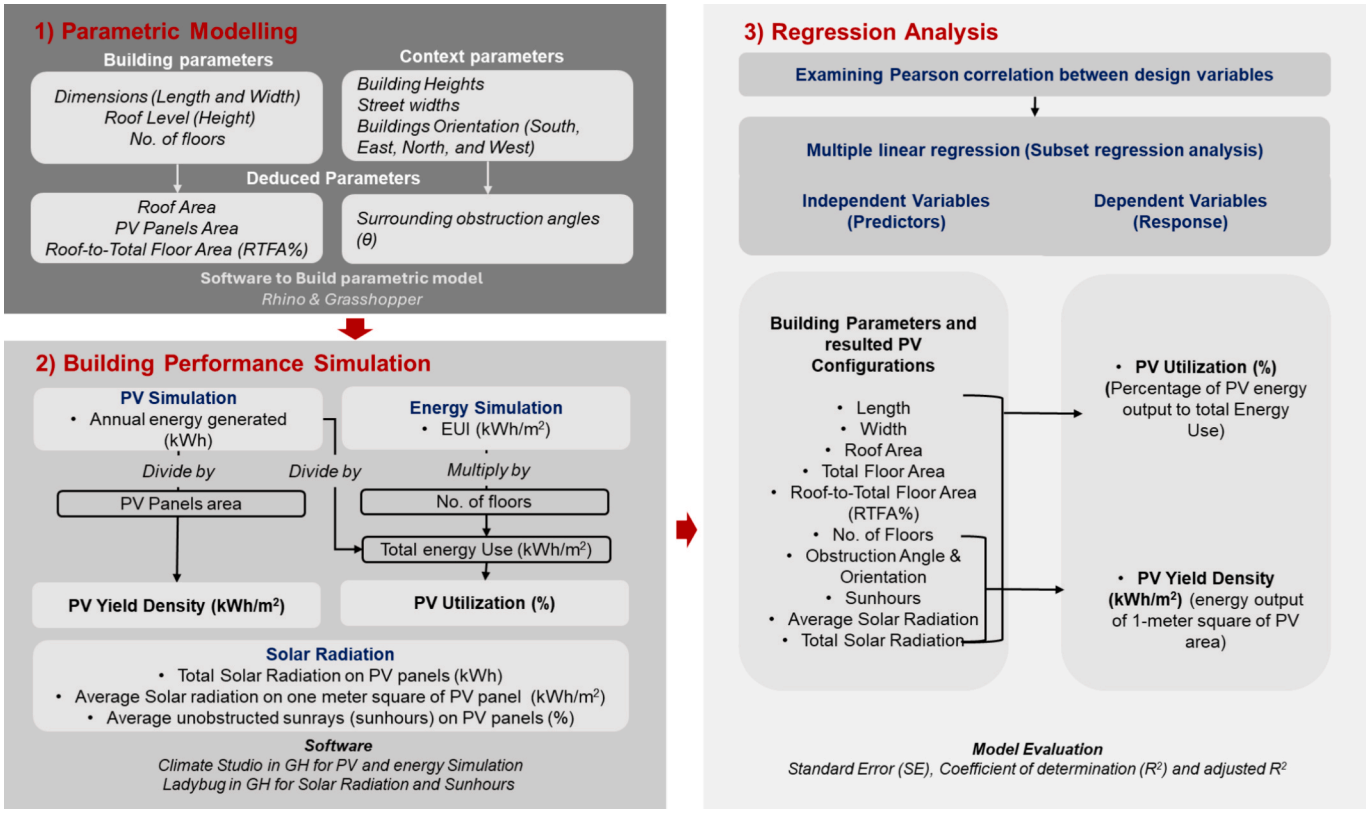

Fig. 1. The workflow for predicting PV Utilization and Yield Density.

surrounded by obstructions from the four orientations. The research explores the impact of varying building configurations and shading patterns on PV Utilization potential and Yield Density. The proposed methodology comprises of three main phases as shown in Fig. 1. The first is concerned with data generation through parametric modelling, incorporating key design variables of building form and surrounded obstructions that impact rooftop PV Utilization potential. The second involves performance simulation analysis for calculating the PV Utilization potential and PV Yield Density. The third step proposes regression models for analyzing the impact of designed variables and predicting the potential outcome. These phases are sequentially integrated to systematically explore the impact of design parameters on PV performance, ensuring a comprehensive and data-driven approach to achieving the study's objectives.

2.1. Data generation through parametric modelling

The parametric modelling process was performed using Rhino and Grasshopper (GH) software, enabling the generation of a wide range of design configurations. Fig. 2 and Table 1 presented the ranges of building and surrounding context input parameters used in the simulations. The building model varied in height, length and width to produce configurations with roof areas ranging from 225 to 2,025 m^2 and number of floors from 2 to 12 floors assuming a fixed floor height of 3 m, providing a roof-to-total floor area (RTFA %) between 8% and 50%.

Fenestration design adopted window-to-wall ratios (WWR) of 0.6 for the North facade, and 0.4 for the remaining orientations, with a maximum module length of 5 m. Simple horizontal shading devices were modeled on South facing windows. External obstructions were modeled on the four orientations, South, West, North and East, to obtain different shading patterns on rooftops. Different combinations of street widths and obstruction heights were varied to simulate a range of obstruction angles. These angles were further formed by the number of floors, as the height difference between building and the opposing building determine the resulting angle. The simulated obstruction angles ranged from 0 to around 80 degrees, with mean values of 33.7 °, 27.6 °, 16.1 °, and 27.7 °, and standard deviation of 32.2 °, 30.5 °, 27.4 °, and 30.7 ° for the South, West, North and East orientations respectively. PV panels were installed on the available rooftop area, oriented to the South with a fixed tilt angle of 30 °, which was found to be an optimal angle for solar radiation in Cairo's climatic context [28]. Each PV module measured 1 m by 2 m with clear distance of 1.7 m between rows to minimize inter row shading.

2.2. PV simulation analysis

In the second step, building performance simulations were carried out to estimate the energy generated by roof mounted PV system, as well as the overall building energy performance in terms of the energy use intensity (EUI). A total of 1,000 simulation runs were performed, representing various combinations of building and context parameters within Cairo. The EPW weather data file was downloaded from the energyplus website and imported to Climate Studio tool which was used for conducting both PV and energy simulations as illustrated in Fig. 3. The typical average efficiency of commercial PV panels ranges from 15 to 20 % [29]. The lower end of this range was selected (15 %) for the simulation setting, as high temperatures, dust, and other environmental factors reduce PV performance in real operating conditions, making it more representative of actual rated efficiencies. This assumption is supported by a recent study evaluating a rooftop PV system installed in Cairo, which reported an average annual system efficiency of 15.8 % [30].

An effective area factor was set to be 80 % to account for additional architectural or service constraints beyond the modelled stair core and inter-row spacing to be in line with the practical roof utilization factors for PVs [31]. The modelled PV areas ranged from 64 to 1,128 m^2 with effective areas between 51 and 902 m^2. This corresponded to utilization factors (UF) of 0.23 to 0.45, which is the ratio of effective PV area to the

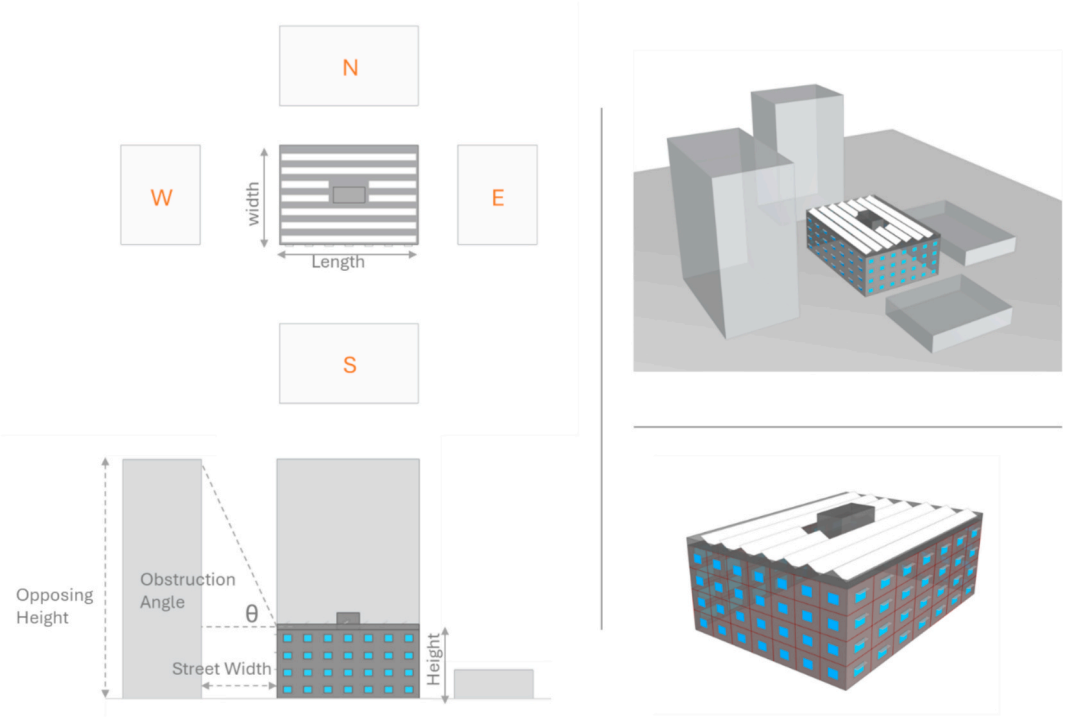

Fig. 2. Building and context design configuration.

Table 1
Parameters range for building and context.

	Building Parameters			Context Parameters
	Roof Height (m)	Length (m)	Width (m)	Obstruction Angle θ (°) and orientation
Range	6–36	15–45	15–45	0–80 S, W, N, E
Increment	3	5	5	Random

total floor area. This aligned closely with the findings of Ghaleb et al. [31] who reported that UF values of office buildings ranged between 0.27 and 0.39. Another study estimated available rooftop area for evaluating PV potential by applying facility coefficients to exclude surfaces which have other specific applications like aerials and HVAC equipment. For 16 representative building typologies, these coefficients ranged from 0.6 to 0.92 with an average of 0.77, indicating an average reduction of 23 % in effective roof area [32]. This closely aligned with the assumed 20% reduction.

The installed PV capacity ranged from 7.7 to 135.4 kW representing the peak direct current output of PV under standard test conditions of solar radiation of 1,000 W/m^2. It was determined based on the effective PV area available on the roof and the assigned PV efficiency (15 %), as expressed in Eq. (1). The implied capacity factor (CF) was then derived to represent the ratio of simulated annual energy output to the theoretical output if the system operated at full capacity over the year, as illustrated in Eq. (2). This factor signified the physical potential of Cairo's climate for energy generation through rooftop PV.

$$PVcapacity = PVeffectivearea \times Solarirradiance\left(1,000\ W/m^2\right) \times PVefficiency \quad (1)$$

$$ImpliedCF = PVenergyoutput[kWh]/(PVcapacity[kW]*8,760) \quad (2)$$

Additionally, Ladybug tool in GH was used to calculate the total and average solar radiation on the PV panels. It was also used to calculate sunhours, defined as the annual duration of unobstructed direct sunlight incident on a surface, derived from the sun position (solar altitude and azimuth) over the year. This metric was referred to as solar access or direct sunlight availability in solar and urban planning studies [33,34] and it can be mathematically expressed by the summation of the sun visibility V(t) over time steps (t) in a year, as illustrated in Eq. (3).

$$Sunhours = \sum_{t=1}^{N} V(t)\Delta t \quad (3)$$

where V(t) is the sun visibility, V(t) = 1, if the sun position at time t is unobstructed by shading, and V(t) = 0, if obstructed. Δt is the time increment (1 h), and N is the total number of analyzed time steps t.

Sunhours was calculated by estimating the annual average number of unblocked sunrays reaching the rooftop PV panels. These sunrays were affected mainly by the four main building obstructions from the four sides, as well as the parapet wall of 1 m height around the perimeter of the roof and stairs core. Sunhours % was then calculated as the percentage of the average unobstructed sunhours to the total possible sunhours, which was derived from the sunpath diagram as shown in Fig. 4.

An automated workflow was developed to run the simulation analysis for around 1,000 design iterations, integrating energy performance simulations within the parametric environment. The resulting data, representing the relationship between design parameters and performance outcomes, were exported to Excel using the Lunchbox *Write to Excel* component in GH for further analysis.

2.3. Developing regression models

The third step involved data analysis to show the relationship between the assigned building and urban variables and both PV Utilization

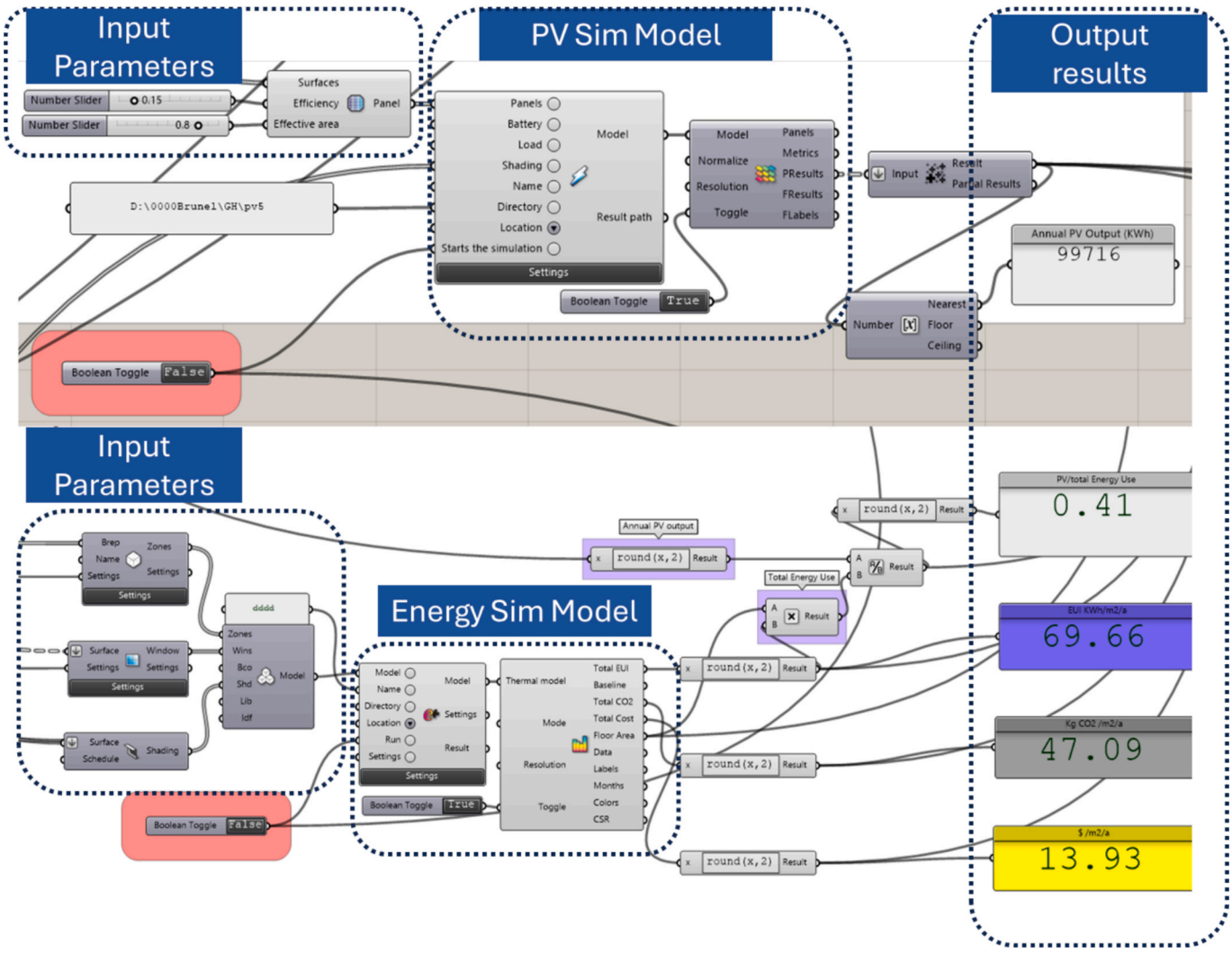

Fig. 3. PV and energy simulation models in Climate Studio in GH.

potential and PV Yield Density. Then, linear and multilinear regression models were developed to predict PV performance. Linear regression models were selected for two main reasons. The primary objective was to develop a simple, interpretable, and easily applicable design tool that can be used to predict PV Utilization and Yield Density without requiring advanced statistical expertise. In addition, preliminary analysis, which included scatterplots and correlation assessments, indicated linear relationships between PV Utilization, Yield Density and building and urban parameters.

The first regression model predicted PV Utilization potential (%), defined as the ratio of PV energy output to total building energy use. The second regression model focused on predicting PV Yield Density, defined as the annual energy generated per one meter square of PV panel. These models captured PV performance and can be used to make predictions, with performance evaluated using Standard Error (SE), Coefficient of determination (R^2) and adjusted R^2 as defined below [35].

Standard error (SE) represents the standard deviation of the prediction errors and provides an interpretation of how spread out these errors are. A lower SE indicates a better fit between predicted and actual values.

$$SE = \sqrt{\frac{SSE}{DFe}} = \sqrt{\frac{1}{n-p-1}\sum_{i=1}^{n}(Y_i - \hat{Y}_i)^2} \tag{4}$$

where SSE is the Sum of Squares of Errors, Dfe is the Degree of freedom which is n-p-1, p is the number of parameters, y_i is the actual or simulated value for a given i and $\hat{y}_i$ is the predicted value for the same i.

The coefficient of determination or R-squared (R^2) quantifies the proportion of variance in the dependent variable that is predictable from the independent variables. It indicates the model's goodness of fit, showing how well the simulated data explains the predicted values when it approaches 1. Adjusted R^2 were used when using multilinear regression as it provides more indicative results when there are multiple variables. R-squared predicted is also calculated which assesses how much the model can predict unseen data.

$$R^2 = \frac{SSR}{SST} = \frac{\sum_{i=1}^{n}(y_i - \hat{y}_i)^2}{\sum_{i=1}^{n}(y_i - \bar{y})^2} \tag{5}$$

$$R^2_{adj} = 1 - \frac{(1-R^2)(n-1)}{n-k-1} \tag{6}$$

Where SSR is the sum of squares of regression, SST is the sum of squares of total, y_i is the actual or simulated value for a given I, $\hat{y}_i$ is the predicted value for the same I, $\bar{y}$ is the average of y, n is the total number of Samples, and k is the number of variables.

Regression models and Pearson correlation analysis were performed using Minitab software which is a statistics software for data analytics and visualizations, while Microsoft excel was used for graphs generation. SPSS was also used for residual diagnostic and applying robust

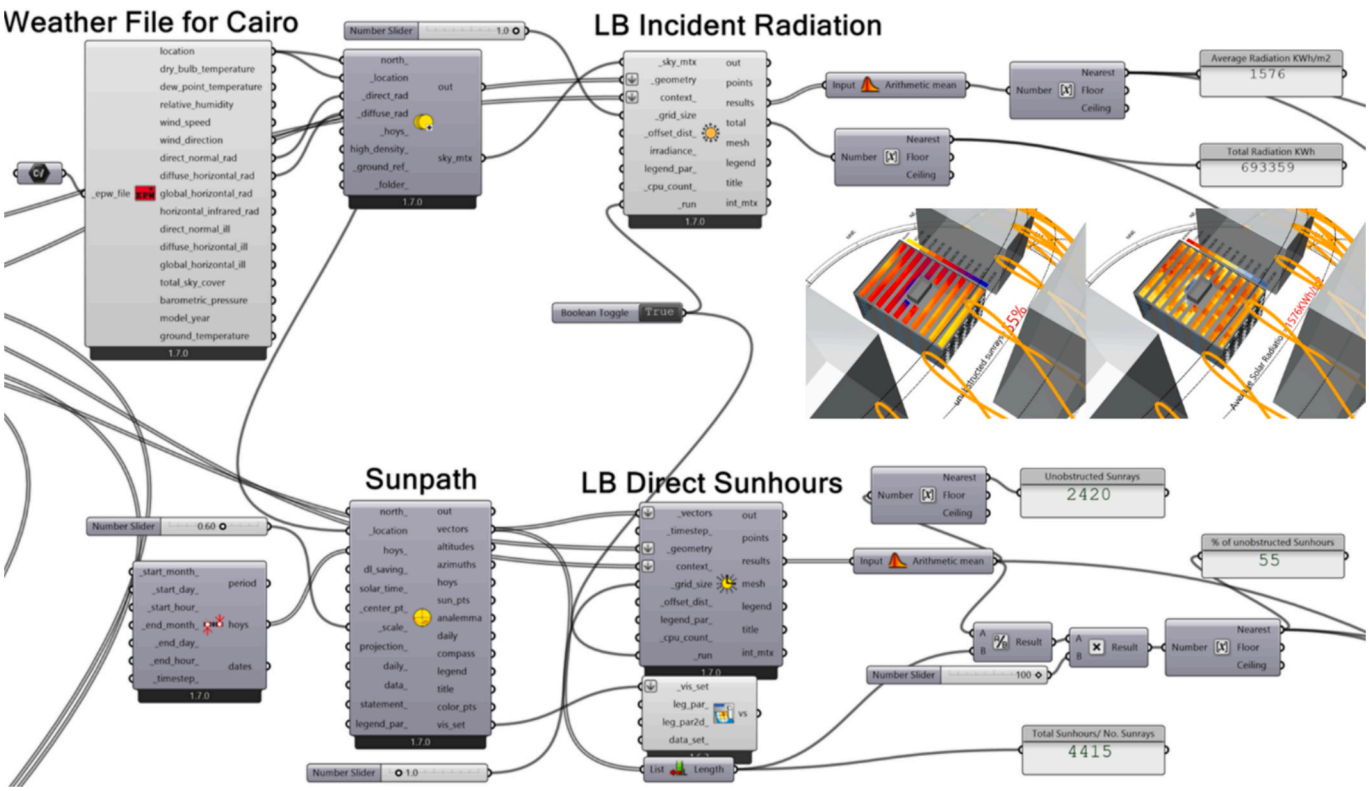

Fig. 4. Solar radiation analysis using Ladybug in GH.

standard errors to ensure unbiased inference using heteroscedasticity-consistent correction (HC3) [36].

Data processing started with a correlation analysis among all variables to identify the existing relationships and avoid problems of multicollinearity and overfitting in the regression model. Subset regression models were applied to find the most influential predictors of PV Utilization and Yield Density while reducing redundancy among correlated variables such as roof area, length and width [37]. This approach allowed for the exploration of different variable combinations, providing a manageable set of variables that maintain high predictive accuracy while avoiding overfitting and multicollinearity. The problem of multicollinearity was detected using Variance Inflation Factor (VIF), which is a factor that quantifies how much variance of an estimated regression coefficient is increased by linear correlation among independent variables. VIF of 1 indicates no correlation, while values above 5 typically suggest a collinearity problem [38].

3. Results and discussion

Results emphasized the significance of considering both building and urban parameters for assessing and predicting the energy performance of roof-mounted PV panels. The analysis was structured into three sections. Section 3.1 examined the simulated results to give insights into the relationship between design variables and PV energy outputs, supported by sample data analysis. Sections 3.2 and 3.3 described the regression models developed for predicting PV Utilization and PV Yield Density, respectively.

3.1. PV simulation analysis

The generated PV energy across all iterations ranged from 13,253 to 260,694 kWh, corresponding to roof areas of 225 m^2 and 2,025 m^2, floor heights of 6 m and 36 m, sun hours of 60 % and 73 %, and average solar radiation levels of 1,668 and 1,815 kWh/m^2, respectively. With PV capacities ranging from 7.7 to 135.4 kW, the corresponding capacity factors ranged between 15 % and 26 %. This range was consistent with the reported actual measures of capacity factors by Edalati et al. [39], which typically ranged between 10 % and 30 %, reflecting fluctuations of weather conditions and daily and monthly variations in solar irradiance. Understanding both the installed PV capacity and the implied capacity factor indicate the realistic productivity of rooftop PV systems. While the described ranges outline the limits of this study, the results reflect that Cairo's climate offers sufficient sunhours and irradiance to make rooftop PV an efficient energy source, while also emphasizing the importance of accounting for building design variables and local obstructions.

3.1.1. Impact of design variables on PV Utilization

To evaluate the contribution of rooftop PV systems to building energy needs, the relationship between PV Utilization and design variables was investigated. Among the tested design variables, the roof-to-total floor area ratio (RTFA %) exhibited a clear and strong relationship with PV Utilization, as shown in Fig. 5. The relationship was approximately linear, with the highest PV Utilization of 125 % reached at an effective area of PV panels of 393 m^2 mounted on a 768 m^2 roof area and RTFA of 50 % without surrounding obstructions, except the parapet wall and stairs core. In contrast, PV Utilization decreased when obstructions were introduced, which is signified by sunhours %. The PV reduction rate was more evident at higher RTFA % indicating an interaction between RTFA % and sunhours %. At same building configuration with RTFA % of 50 % the introduction of obstruction reduced sunhours to 65 %, resulting in a notable decline in PV Utilization (from 125 % to 70 %). This demonstrated that maximizing rooftop PV potential depends not only on the RTFA % but also managing surrounding obstructions and shading patterns. Therefore, evaluating the magnitude of this impact is crucial for informed decision-making in PV installation.

To better illustrate this observation with a qualitative illustration, a representative data sample of the typical performance shown in Fig. 6 was analyzed to find the relationship between PV Utilization and the design variables: RTFA % and sunhours %. It was then quantified

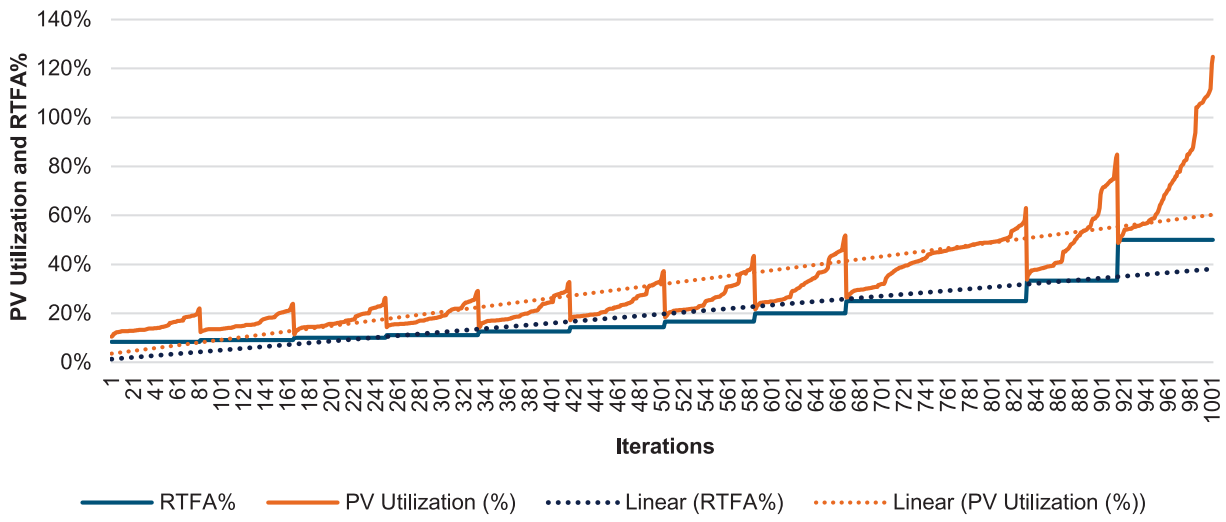

Fig. 5. The relation between RTFA % and PV Utilization.

through regression analysis of the full dataset to demonstrate the overall relationship. This sample was chosen with the same roof area of 625 m^2 to isolate the area effect, which also reflected the mean value of simulated roof areas. The roof-to-total floor area (RTFA %) showed a clear positive correlation with PV Utilization. The average solar radiation and sunhours % were correlated positively with each other; however, they did not show a consistent relation with the PV Utilization, unlike RTFA %. Discrepancy was shown in Fig. 6 where the PV Utilization increased with the decrease of radiation and sunhours %, and vice versa. This returned to variables interaction, where RTFA % had more dominant influence on PV Utilization. On the other hand, sunhours had a noticeable impact on PV Utilization when comparing cases with the same RTFA %, highlighting the significance of the impact of external obstruction. For example, by comparing the cases 1 and 7, each having the same RTFA of 50 %, the PV Utilization declined by 31 % through the effect of obstructions and reduction of sunhours %. In case 1, with no obstructions and sunhours of 90 %, average solar radiation reached 2,224 kWh/m^2 and PV Utilization reached 112 %, exceeding the building's energy use by 12 %. When adding obstructions as in case 7, with sunhours 61 %, the average solar radiation decreased to 1,700 kWh/m2, and PV Utilization declined by 31 % (from 112 % to 81%). This impact of sunhours % on PV Utilization was less significant at lower RTFA %. For instance, in cases number 6 and 12, which had RTFA of 8 %, and nearly the same sunhours variation (90 % to 64 %) as cases 1 and 7 (90 % to 61 %), PV Utilization declined by only 5 % (from 20 % to 15 %). These sample results suggest that the impact of obstructions on PV Utilization may vary with RTFA %, with a stronger influence observed at higher RTFA % values. Therefore, further analysis on a larger dataset was needed to validate and better understand this relationship.

To validate this relationship, cases with the highest and lowest RTFA % (50 % and 8 %) were plotted in Fig. 7a to examine the effect of sunhours % on PV Utilization. The graph confirms a significant impact of surrounding obstructions on PV Utilization at high RTFA of 50 %. The trendline showed a steep slope of 1.0834, indicating high sensitivity of

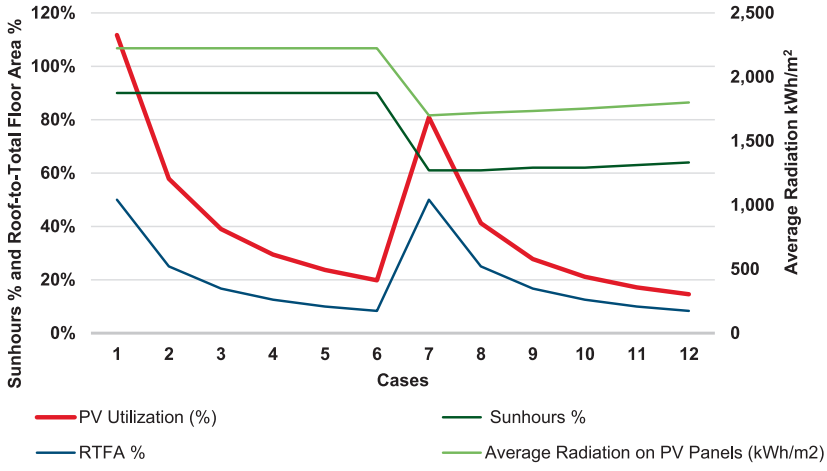

Case No.	RTFA %	Average Radiation on PV Panels (kWh/m^2)	Sunhours % (unobstructed sun rays)	PV Utilization (%) (PV Energy output/T. Energy Use)
1	50	2,224	90	112
6	8	2,224	90	20
7	50	1,700	61	81
12	8	1,800	64	15

Fig. 6. A sample of data showing the relation between PV Utilization and predictable variables.

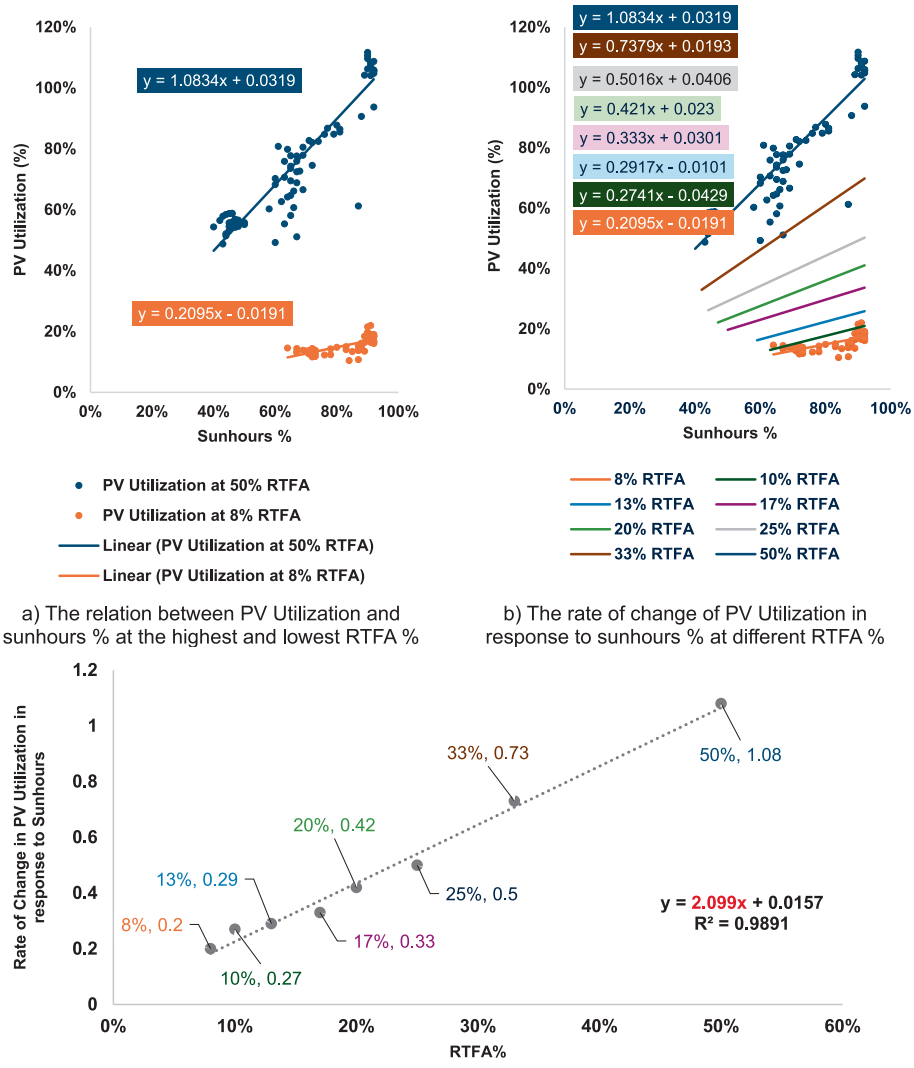

a) The relation between PV Utilization and sunhours % at the highest and lowest RTFA %

b) The rate of change of PV Utilization in response to sunhours % at different RTFA %

c) The impact of RTFA % on the sensitivity of PV Utilization to variations in Sunhours %

Fig. 7. The relationships between RTFA % and sunhours % on PV Utilization.

PV Utilization to reductions in sunhours. In contrast, this impact decreased at low RTFA % of 8 % with the trendline slope decreasing to 0.2095. To further quantify the relationship, PV Utilization was analyzed across the full RTFA % range (50% to 8%) as shown in Fig. 7b. The results showed a strong linear relation (R^2 of 0.99), where the influence of sunhours on PV Utilization almost doubled (coefficient = 2.099) with each incremental increase in RTFA % as shown in Fig. 7c. This highlighted the significant impact of RTFA % on the sensitivity of

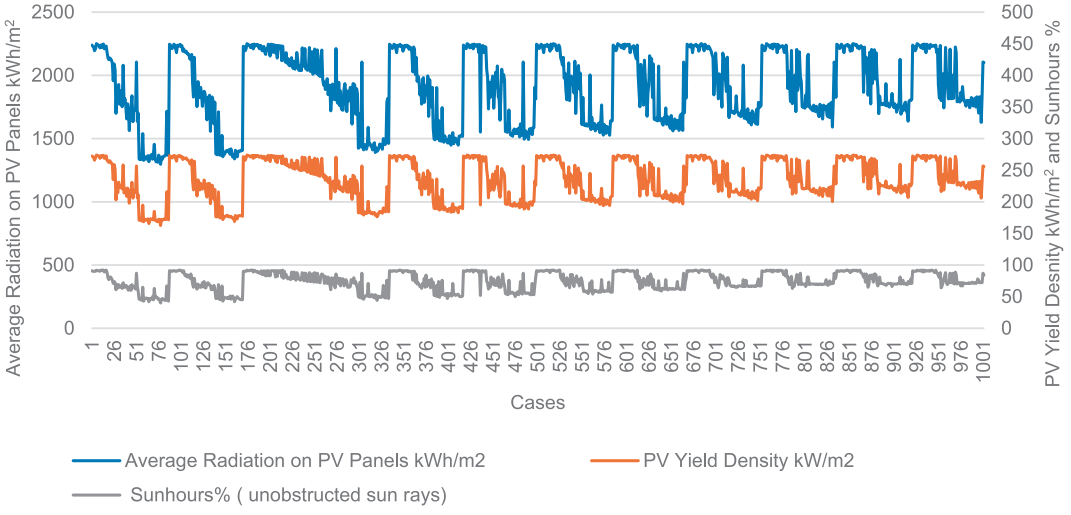

Fig. 8. The relation between PV Yield Density and average radiation and Sunhours %.

PV Utilization to variations in sunhours %, thus signifying the interactive effect of building design (RTFA %) and urban morphology (sunhours %).

3.1.2. Impact of design variables on PV yield density

PV Yield Density was the second metric investigated to evaluate PV energy performance. It represented the average PV energy generated per square meter of PV area. It ranged from 162 to 274 kWh/m^2, with average incident radiation on PV panels ranging from 1,297 to 2,251 kWh/m^2 and sunhours % between 40 % and 92 %. These variations in PV Yield Density were primarily driven by sunhours %and solar radiation, with a clear linear relationship observed between them, as shown in Fig. 8.

To visualize and interpret representative results, Table 2 presented two configurations of surrounding building obstructions and their respective effect on sunhours % and solar radiation and overall PV performance. This comparison provided qualitative insights that were then quantified through regression analysis. In both scenarios, PV panels were installed on a roof area of 875 m^2, with an effective PV area of 346 m^2 and RTFA of 17 %. The obstruction angles differed, resulting in average annual solar radiation of 1,887 kWh/m^2 in the first case and 1,576 kWh/m^2 in the second reflecting mean values across the dataset. Correspondingly, the sunhours % (unobstructed sunrays) were reduced from 68 % to 55 %. As a result, PV Yield Density decreased by 67 kWh/m^2 (from 266 kWh/m^2 to 199 kWh/m$^{2)}$. Both PV Yield Density and Utilization were affected by surrounding obstructions from the South, West, and East orientations, with sunhours % serving as the key mediating factor. These findings highlighted the significant influence of obstruction angles on solar access and hence on PV performance. To further investigate this effect on a larger scale, regression analysis was then performed.

Table 2
The effect of surrounding obstructions on solar radiation and sunhours % on PV performance.

Geo. parameters	Length	Width	No. of Floors	Roof-to-Total Floor Area (RTFA%)
	25	35	6	17

Obstruction Angles (°)	South	East	North	West	South	East	North	West
	0	79	77	0	69	50	0	69

Average solar Radiation (kWh/m^2)	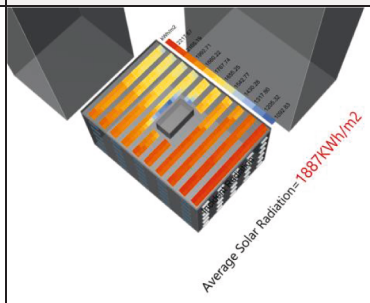	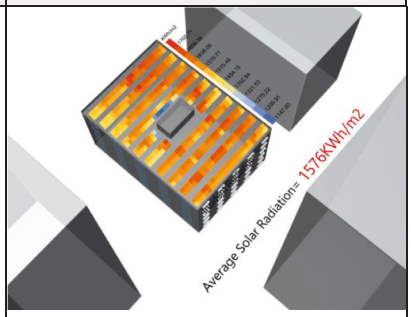
	1,887	1,576
Sunhours (%)	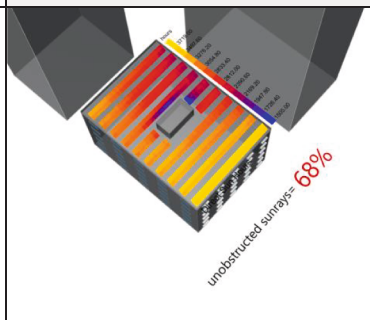	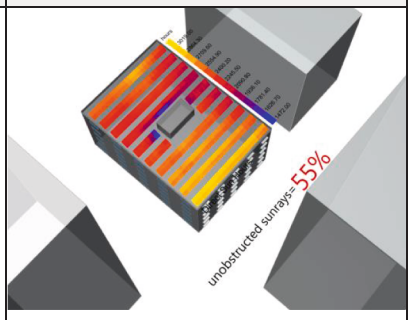
	68	55
EUI (kWh/m^2)	70.02	74.85
PV energy Output/year (kWh)	97,635.75	85,843.23
PV Utilization (%)	27	22
PV Yield Density (kWh/m^2)	266	199

3.2. Regression model for predicting PV utilization

The first step in the multi regression involved examining Pearson correlation between design variables as shown in Fig. 9. PV Utilization showed a high positive correlation with both the number of floors (0.8) and the roof-to-total floor area RTFA % (0.89) indicating their potential effectivness in the regression model. However, these two dependant variables were also highly negatively correlated with each other (−0.88), which indicated multicollinearity. In addition, the multi regression model showed a moderate Variance Inflation Factor (VIF) of 4.33, indicating the potential of unreliable coefficient estimates. To address this, a linear regression model was done for RTFA % given its higher correlation value with PV potential. The model yielded adjusted R^2 of 78.82 % and predicted R^2 of 78.64 %, with standard error of 8.88 %. However, this model, graphically represented in Fig. 10, accounted only for the building configuration without taking into consideration the urban context and its shading impact.

To get a more comprehensive model, a subset regression analysis was

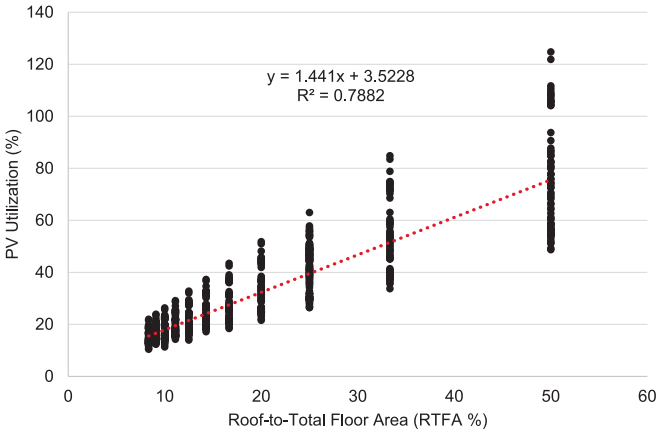

Fig. 10. A simple linear regression model for predicting PV Utilization.

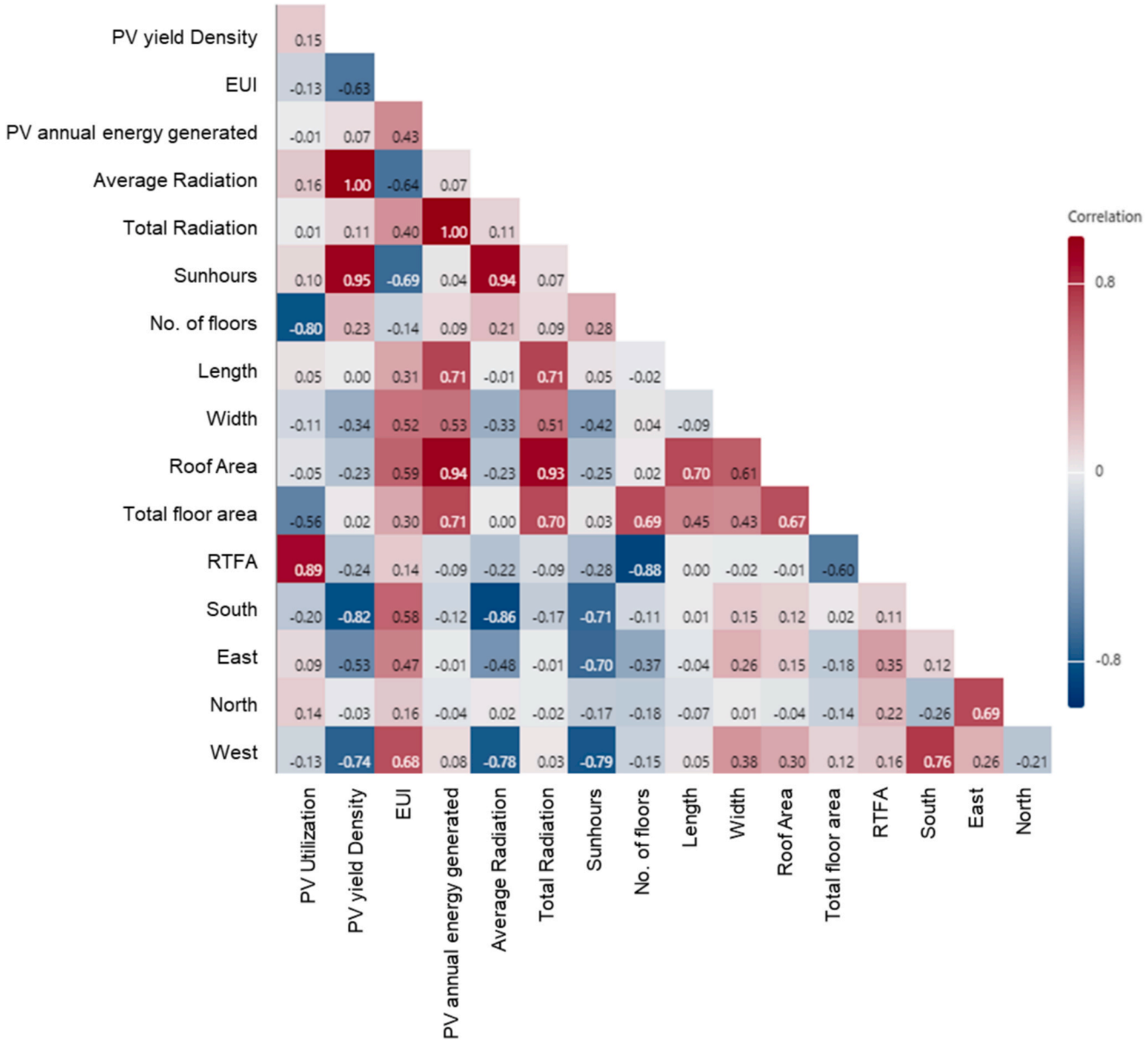

Fig. 9. A correlation analysis between all variables.

Table 3
A subset regression model for PV Utilization potential using 13 independent variables.

No. of Variables	R-Sq	R-Sq (adj)	R-Sq (pred)	SE	Average Radiation kWh/m^2	Total Radiation kWh	Sunhours %	No. of Floors	Length	Width	Roof Area	Total Floor Area	RTFA %	South	East	North	West
1	78.4	78.4	78.6	8.88									X				
1	63.8	63.8	63.6	11.62				X									
2	**92.1**	**92.1**	**92.0**	**5.44**	**X**								**X**				
2	**91.8**	**91.8**	**91.7**	**5.53**			**X**						**X**				
3	92.8	92.8	92.7	5.17	X								X			X	
3	92.7	92.7	92.6	5.23	X								X		X		
4	93.1	93.1	93.0	5.07	X			X					X		X		
4	93.1	93.1	93.0	5.07	X			X					X			X	
5	93.5	93.5	93.4	4.93	X	X		X					X		X		
5	93.5	93.4	93.3	4.94	X			X			X		X		X		
6	93.7	93.6	93.5	4.87	X			X	X	X			X		X		
6	93.6	93.6	93.5	4.88	X	X		X					X	X			
7	93.9	93.8	93.7	4.79	X			X	X	X	X		X		X		
7	93.8	93.7	93.6	4.83	X	X		X	X	X			X		X		
8	93.9	93.9	93.8	4.77	X			X	X	X	X		X	X	X		
8	93.9	93.9	93.7	4.78	X			X	X	X	X		X		X		X
9	94.0	93.9	93.8	4.74	X		X	X	X	X	X		X		X		X
9	94.0	93.9	93.8	4.76	X			X	X	X	X		X	X	X	X	
10	**94.0**	**94.0**	**93.9**	**4.74**	**X**		**X**	**X**	**X**	**X**	**X**		**X**		**X**	**X**	**X**
10	94.0	93.9	93.8	4.74	X		X	X	X	X	X		X	X			X
11	94.0	94.0	93.8	4.73	X		X	X	X	X	X	X	X		X	X	X
11	94.0	94.0	93.8	4.74	X		X	X	X	X	X		X	X	X	X	X
12	94.0	94.0	93.8	4.74	X		X	X	X	X	X	X	X	X	X	X	X
12	94.0	94.0	93.8	4.74	X	X	X	X	X	X	X	X	X		X	X	X
13	94.0	94.0	93.8	4.74	X	X	X	X	X	X	X	X	X	X	X	X	X

then performed using the 13 independent variables: average solar radiation, total solar radiation, Sunhours %, number of floors, building length, width, roof area, total floor area, roof-to-total floor area RTFA %, South, East, North, and West angles. This approach minimized information loss and facilitated a comparative analysis of various subsets of predictor variables. The optimal subset was selected aiming to maximize adjusted R^2 adjusted while minimizing overfitting and multicollinearity.

In the subset regression analysis presented in Table 3, a total set of 25 models were explored, each composing of a different combination of variables (X) ranging from 1 to 13 providing the two best performing models for each variable number. This allowed comparing and selecting the lowest number of independent variables that maintain a high predictive power to avoid overfitting. A notable improvement was found in model accuracy by adding the average radiation as a second variable with the RTFA %. Despite its low individual correlation with the PV Utilization ($p < 0.2$), it increased the adjusted R^2 to 92.1 % and predicted R^2 to 92 %, while decreasing standard error to 5.44 %.

When replacing average radiation with sunhours %, a slight difference was observed, where both variables demonstrated high predictive performance as highlighted in Table 4. These variables reflected the influence of urban context and the associated shading effects. The second model, using sunhours %, was advantaged despite performing slightly lower compared to the average radiation model, as sunhours % can be claculated direclty without the need for simulation, unlike the solar radiation. They can be simply estimated by identifying the number of sunrays passing through the surrounding building obstructions and reaching the rooftop.

When adding more variables, the model's performance was not found to have a significant increase. It peaked with an adjusted R^2 of 94 % and predicted R^2 of 93.9 % when at least 10 variables were included as highlighted in Table 3. With this large number of variables, a problem of overfitting and multicollinearity may occur, particularly among correlated variables like length, width and roof area which require another method like using Principle Component Regression (PCR) to reduce model complexity [40].

Therfore, the two-variable regression model (RTFA % and sunhours %) was selected, achieving adjusted R^2 of 91.8 % and predicted R^2 of 91.7 %, and a standard error of 5.53 %. The variation inflation factor (VIF) was low at 1.08 confirming the absence of multicollinearity between the two variables. The regression coefficients of the two variables demonstrated the relative impact of each variable showing a higher impact for the RTFA % of coefficient 1.61, while sunhours % of coefficient 0.51 ($p < 0.001$). The ANOVA results showed that the regression model is highly significant ($F = 5{,}598.257$, $p < 0.001$), indicating that the predictor variables (RTFA % and Sunhours %) explain a large proportion of the variance in PV Utilization as shown in Table 4.

When observing the residual plot, heteroscedasticity was indicated, as the variance of residuals changed across the range of predicted values. At lower predicted values the residuals were tightly clustered, while at higher predicted values, the residuals showed a fanning pattern with large positive and negative deviations. Accordingly, robust standard errors were applied to ensure unbiased inference using heteroscedasticity-consistent correction (HC3) which adjusts the standard errors by giving more weight to observations with large influential points without changing the coefficients. The resulting 95 % confidence intervals were narrow, and all coefficients remained highly significant ($p < 0.001$), indicating stable and reliable parameter estimates as shown in Table 5.

3.3. Regression model for predicting PV yield density

PV Yield Density is the second objective investigated in this study, indicating the annual PV energy output per square meters. Results showed high positive correlations with average radiation (1.00) and sunhours % (0.95), and high negative correlation with South (−0.82) and West angle (−0.74), as well as a moderate negative correlation with

Table 4
The selected multi regression model results for the PV Utilization and ANOVA analysis.

Regression Equation

PV Utilization (%) = −37.51 + **0.5075** Sunhours % + **1.6110** RTFA %

Model Summary

SE	R-sq	R-sq(adj)	R-sq(pred)
5.53	91.81%	91.79%	91.71%

ANOVA

	df	SS	MS	F	Significance F
Regression	2.000	342,538.651	171,269.326	5,598.257	0.000
Residual	999.000	30,562.737	30.593		
Total	1,001.000	373,101.389			

Table 5
Residual plot and robust standard errors of PV Utilization model.

Residual plot

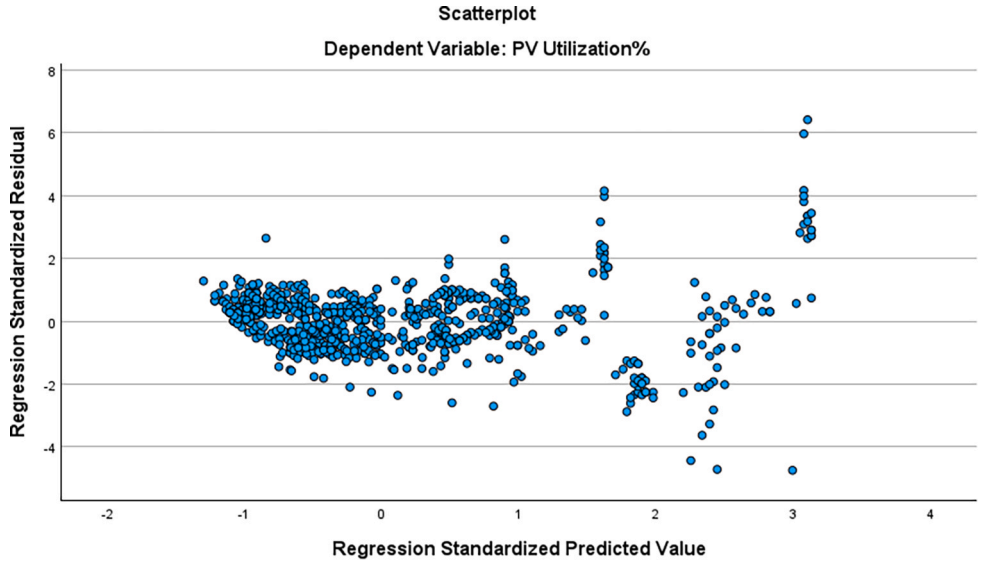

Parameter Estimates with Robust Standard Errors

Dependent Variable: PV Utilization

Parameter	Coefficient (β)	Robust Std. Error[a]	t	P- value	95% Confidence Interval	
					Lower Bound	Upper Bound
Intercept	−37.549	1.583	−23.715	<0.001	−40.656	−34.442
RTFA %	1.614	0.030	53.270	<0.001	1.554	1.673
Sunhours %	0.508	0.017	29.636	<0.001	0.474	0.542

a. HC3 method.

Table 6
The best subset regression analysis for PV Yield Density.

No. of Variables	R-Sq	R-Sq (adj)	R-Sq (pred)	SE	Sunhours %	South	East	West
1	**90.6**	**90.5**	**90.5**	**9.88**	**X**			
1	67.0	67.0	66.9	18.49		X		
1	55.2	55.2	55.0	21.54				X
1	27.7	27.7	27.5	27.35			X	
2	**94.8**	**94.8**	**94.8**	**7.33**	**X**	**X**		
2	94.2	94.2	94.2	7.75	X		X	
2	90.6	90.5	90.5	9.89	X			X
2	85.7	85.7	85.6	12.17		X	X	
3	97.1	97.1	97.1	5.47	X		X	X
3	96.2	96.2	96.2	6.28	X	X		X
3	95.1	95.1	95.1	7.10	X	X	X	
3	86.2	86.2	86.1	11.95		X	X	X
4	**98.0**	**98.0**	**98.0**	**4.55**	**X**	**X**	**X**	**X**

East angle (−0.53). Notably, these variables were also correlated with each other, indicating the occurrence of multicollinearity. As shading-related variables were the dominant drivers of PV Yield Density, the regression model focused on obstruction angles and sunhours % while excluding other variables with weak contributions and low correlation to ensure statistically robust and meaningful predictors. The average radiation was intentionally excluded as it requires simulation process to obtain its value. The focus of this phase was on finding the influence of building and urban morphology parameters on PV Yield Density using variables accessible at the early design stage. Linear regressions were then performed using each of the remaining variables individually, as well as in the best subsets, as shown in Table 6. Model performance was evaluated aiming to maximize adjusted R^2 while minimizing VIF.

The highest R^2 was achieved when including all variables, reaching 98 %. However, the model showed critically high VIF of 14.72, as shown in Table 7, indicating severe multicollinearity and thus unreliable coefficient estimates. The simple linear model with sunhours % as the independent variable explains 90.5 % of the variability in PV Yield Density, with an intercept of 75.8 and a coefficient of 2.14 for sunhours %. However, adding the South angle to the model increased R^2 by 4.3 %. This improvement can be attributed to the critical role of South orientation in Cairo, as rooftop PV panels oriented South receive the highest solar radiation due to exposure to high altitude sun angles, thereby improving prediction accuracy. Moreover, sunhours % act as a mediating factor for obstructing angles around the building, improving model's predictive accuracy compared to using obstruction angles alone. When only the South, West and East obstruction angles were included, the prediction model reached a maximum R^2 of 86.2 % as shown in Table 6. In contrast, using sunhours % alone increased accuracy with 4.4 %, reaching R^2 of 90.6%. This signified the practical value of incorporating sunhours %, even as a derived parameter, to enhance model prediction for rooftop PV design. Accordingly, the best compromise between model fit and multicollinearity was obtained with a two-variable model (sunhours % and South angle), as illustrated in Table 8, which reached R^2 of 94.8 % and VIF of 2. Sunhours % had the strongest effect with a coefficient of 1.611, followed by South angle with coefficient of 0.508 ($p < 0.001$). The ANOVA results showed that the

Table 7
Multi regression model for PV Yield Density using all four variables showing high VIF.

Term	Coefficient	VIF
Constant	1.83	
South Angle	−0.19727	4.38
East	0.3351	5.69
West	0.37595	4.45
Sunhours %	2.9650	14.72

Table 8
The selected multi regression model for PV Yield Density and ANOVA analysis.

Regression Equation

PV Yield Density (kWh/m^2) =120.07–0.291 South Angle + 1.68 Sunhours %

Model Summary

SE	R-sq	R-sq(adj)	R-sq(pred)
7.33812	94.81%	94.80%	94.78%

ANOVA

	df	SS	MS	F	Significance F
Regression	2	981,956.9	490,978.4	9,117.856	0
Residual	999	53,794.17	53.848		
Total	1001	1035,751			

Table 9
Residual plot and robust standard errors of PV Yield Density model.

Residual plot

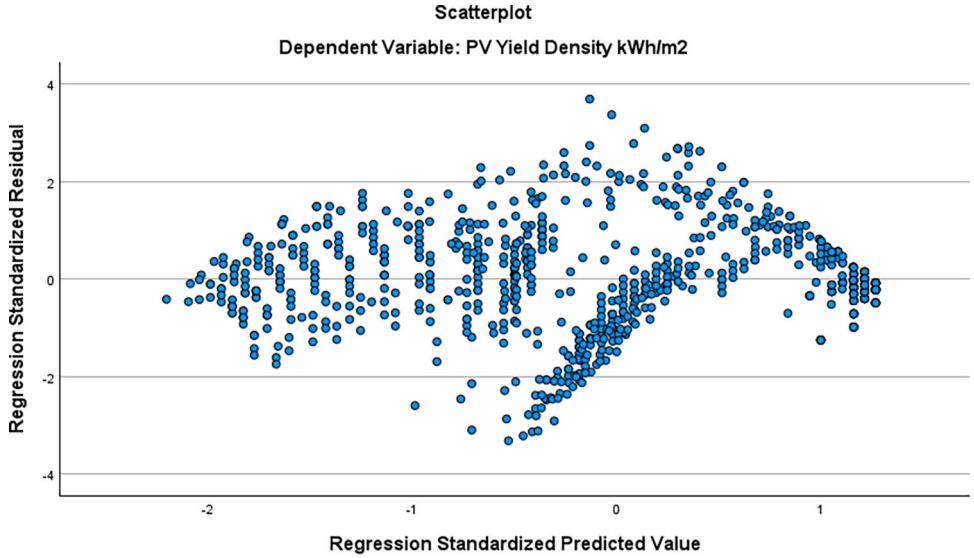

Parameter Estimates with Robust Standard Errors

Dependent Variable: PV Yield Density kWh/m^2

Parameter	Coefficient (β)	Robust Std. Error[a]	t	P-value	95% Confidence Interval	
					Lower Bound	Upper Bound
Intercept	120.108	2.218	54.141	<0.001	115.755	124.461
Sunhours %	1.679	0.025	67.797	<0.001	1.631	1.728
South	−0.291	0.012	–23.392	<0.001	−0.315	−0.266

a. HC3 method.

Table 10
ANOVA of sunhours % model.

ANOVA					
	df	SS	MS	F	Significance F
Regression	3	190,159.7	63,386.57	4,564.431	0
Residual	998	13,859.3	13.88707		
Total	1001	204,019			

regression model was highly significant ($F = 9{,}117.856$, $p < 0.001$), indicating that the predictor variables (Sunhours % and South angle) explain a large proportion of the variance in PV Yield Density. Robust standard errors were applied using HC3 to ensure unbiased statistical inference, and the 95 % confidence intervals showed narrow bounds, indicating stable coefficient estimates as shown in Table 9.

This model can be applied in the early design phase to estimate the Yield Density potential of installing PV panels on the roof based on surrounding contextual parameters. It supports the decision making by indicating the required PV area to be installed to achieve a target energy output. Beyond building energy use, this model provides an overview of roof potential under varying shading patterns and relates the energy generated to the PV area or number of panels installed.

To conclude, in both regression models for PV Utilization and PV Yield Density, sunhours % was found to be a critical predictor of PV performance. Sunhours % was derived from the sun path diagram and obstructions causing shade on the PV panels, like the stairs core and parapet wall. In this study, such elements blocked between 2 % and 11 % of the sunrays reaching the PV panels, depending on the roof area. More substantial reductions in sunhours % were caused by external surrounding obstructions with values decreasing to as low as 40 % in cases of high obstruction angles in the South, East and West.

To estimate the sunhours % without the need of specific tools for sunpath, it was advantageous to develop a mathematical model that calculates sunhours % from obstruction angles or street width and building and obstruction height difference. An additional regression model was therefore developed to obtain the sunhours % from the obstruction angles of South, East and West, while excluding the north which had a negligible effect on reducing sunhours %. The resulting model achieved a high adjusted R^2 of 93.19 % and SE 3.7 % as expressed in the equation below.

$$Sunhours\% = 91.573 - 0.16264\ South(\theta) - 0.25959\ East(\theta) - 0.16825\ West(\theta) \quad (7)$$

$$\theta = \arctan\left(\frac{Height\ difference}{Street\ Width}\right) \times \frac{180}{\pi} \quad (8)$$

The regression model explained a high proportion of variance in sunhours % as indicated by a highly significant F-statistic ($F = 4{,}564.431$), with low residual mean square ($MS = 12.89$) signifying limited unexplained variance as shown in Table 10. To address heteroscedasticity, identified in the non-constant variance shown in the residual plot (Table 11), HC3 robust standard errors were applied. The estimates showed that obstruction angles had a statistically significant effect on Sunhours % ($p < 0.001$). The East obstruction angle showed the strongest reduction effect with a coefficient of − 0.260, followed by the West (−0.168) and South (−0.163). This suggested that obstructions from the South have the lowest impact on annual sun exposure for the studied rooftop configurations, which is consistent with Cairo's solar path, where the sun has high altitude angles in the southern sky, while lower altitude angles in the East and West making solar access more

Table 11
Residual plot and robust standard errors of sunhours % model.

Residual plot

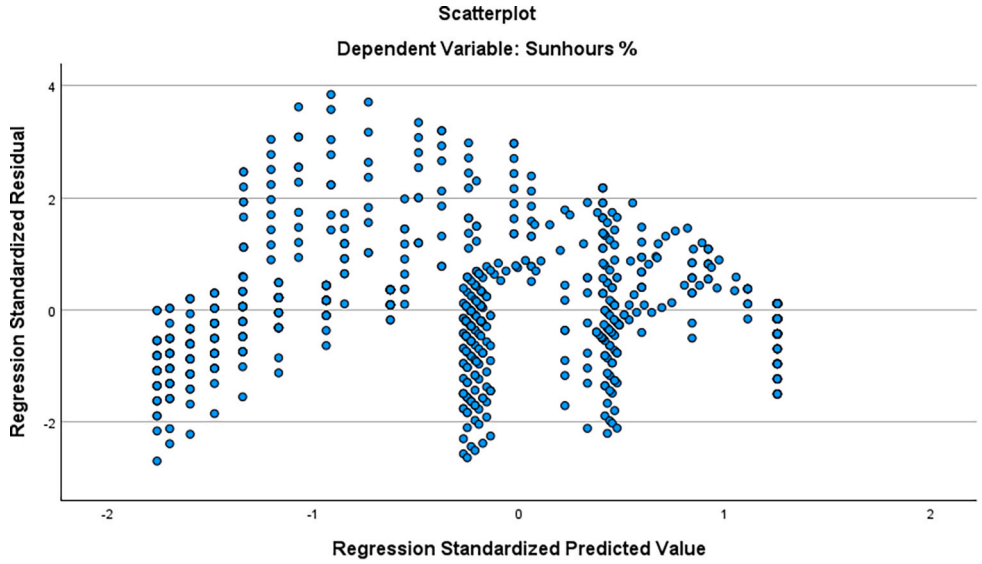

Parameter Estimates with Robust Standard Errors
Dependent Variable: Sunhours %

Parameter	Coefficient (β)	Robust Std. Error[a]	t	P-Value	95% Confidence Interval	
					Lower Bound	Upper Bound
Intercept	91.573	0.120	764.262	<0.001	91.338	91.808
South	−0.163	0.005	−30.719	<0.001	−0.173	−0.152
East	−0.260	0.005	−56.999	<0.001	−0.269	−0.251
West	−0.168	0.006	−30.540	<0.001	−0.179	−0.157

a. HC3 method.

sensitive to obstructions. The model intercept of 91.57 % represented the expected annual sunhours % in the absence of external obstructions, while the remaining 8.43 % reduction was attributed to shading from the parapet wall and stairs core.

The developed predictive regression models provide rapid and resource-efficient estimates of PV Utilization and PV Yield Density with the least possible resources. They address a key limitation in previous research by providing simple, practical calculations that capture the impact of building and urban morphology using basic geometric parameters of building length, width, height, surrounding building heights, orientation and street widths. Using these models, sunhours %, RTFA %, and obstruction angles can be derived and then used to predict PV Utilization and Yield Density. These models bridge a critical gap by providing straightforward, early-stage assessment of rooftop PV potential. Moreover, the regression equations have been integrated into a user-friendly web-based tool that allows users to obtain results instantly without making any calculation, which is accessible through this link: Solar Potential Tool · Streamlit.

4. Conclusions

Climate change and global warming require urgent attention from all entitles and individuals as all share the responsibility in addressing their causes and mitigate their consequences. This global problem urges everyone to contribute to achieving sustainable development goals, particularly in advancing renewable energy adoption. In cities like Cairo, where solar radiation is abundant, it is essential to assess the potential benefits and utilization of solar energy through the available technologies. Roof-mounted PV panels are one of the most widely deployed solutions. However, their effectiveness can vary based on climatic, urban, technical and economic factors.

This study makes a significant contribution by integrating urban and environmental parameters within a parametric modelling framework, enabling the evaluation of rooftop PV performance in terms of Utilization potential and Yield Density. The novelty lies in bridging architectural design considerations with quantitative PV performance simulation, offering a methodology that can inform early-stage design decisions to maximize renewable energy potential. The developed regression models are designed to be user-friendly, providing straight forward insights into how building geometry and shading from external obstructions influence PV potential and subsequent energy savings. This dimension is often overlooked despite having a great influence on the performance of rooftop mounted PV panels. Accounting for these factors through regression models highlights the importance of orientation and shading control in design and planning decisions for maximizing the benefits of solar potential. Key findings include:

- PV systems can supply up to 125 % of a building's total energy requirements at a Roof-to-Total Floor Area (RTFA %) of 50 % with no external obstructions and sunhours of 91 %.
- By decreasing sunhours to 65 % for the same building configuration, PV Utilization decreased from 125 % to 70 %, signifying the impact of obstructions.
- The effect of sunhours % is diminished at lower RTFA % signifying the major role of RTFA % in determining PV Utilization potential.
- As rooftops occupy a larger proportion of building area (High RTFA %), PV systems become more sensitive to reductions in sunhours %. For every increase in RTFA %, the sensitivity of PV Utilization to sunhours % doubles, emphasizing their interdependence.
- Sunhours % is a key predictor for both PV Utilization and PV Yield Density acting as a mediating variable that captures the influence of obstruction angles. Its inclusion significantly enhances the model's predictive accuracy compared to models based only on obstruction angles.
- The South obstruction angle is the most influential supplementary variable when combined with sunhours %, improving the PV Yield Density model R^2 from 90.5 % to 94 % without introducing problems of multicollinearity.
- The sunhours % model indicates that 91.57 % of sunrays reach the rooftops in the absence of obstructions, excluding shading from building's parapet wall and stairs core.

These findings reinforce the need to consider urban morphology and environmental parameters as integral components of rooftop PV planning and design, providing a quantitative foundation for future decision-making frameworks aimed at maximizing solar energy potential in dense urban contexts. It can provide urban planners, architects, and policymakers with evidence-based insights to guide the design of building codes, incentive schemes, and rooftop planning policies that align both environmental and spatial factors to accelerate renewable energy adoption. Although, the study is confined to the hot arid climate of Cairo, Egypt, future research could extend this methodology to other climatic contexts allowing for broader applicability across different urban settings. In addition, machine learning techniques could be employed to further enhance prediction accuracy and scalability.

CRediT authorship contribution statement

Fatma Fathy: Writing – original draft, Methodology, Investigation, Formal analysis, Conceptualization. **Rabee Shamass:** Writing – review & editing, Supervision. **Xiangming Zhou:** Writing – review & editing, Supervision, Conceptualization.

Declaration of competing interest

The authors declare that they have no known competing financial interests or personal relationships that could have appeared to influence the work reported in this paper.

Acknowledgement

This research is part of the ISPF Early Career Fellowship Scheme – Egypt, sponsored by the British Council through the International Science Partnerships Fund. It falls under the sub-project titled "Nurturing Early Career Fellows in Climate Resilient and Sustainable Built Environment Research Agenda".

The authors would like to thank Dr. Mohamed Anwar for his technical assistance in the development of the web-based tool.

Data availability

Data will be made available on request.

References

[1] I.E.A. IEA, Energy Efficiency 2023 (2023).
[2] IRENA, Global energy transformation: A roadmap to 2050 (2019 edition), Abu Dhabi., (2019).
[3] IRENA, Renewable energy in climate change adaptation: metrics and risk assessment framework, Abu Dhabi, 2025.
[4] Y. Wu, Z. Liu, J. Liu, H. Xiao, R. Liu, L. Zhang, Optimal battery capacity of grid-connected PV-battery systems considering battery degradation, Renew. Energy 181 (2022) 10–23, https://doi.org/10.1016/j.renene.2021.09.036.
[5] O.O. Yolcan, World energy outlook and state of renewable energy: 10-Year evaluation, Innov. Green Develop. 2 (4) (2023) 100070, https://doi.org/10.1016/j.igd.2023.100070.
[6] P.R.S. REN21, Renewables 2022 global status report, Renewable Energy Policy Network for the 21st Century (REN21), (2022).
[7] IEA, Carbon-Free Electricity in G20 Countries, (2025).
[8] NREA, Annual Report 2024, New & Renewable Energy Egyptian Authority, Egypt, (2024).
[9] P. Kosmopoulos, S. Kazadzis, H. El-Askary, The solar Atlas of Egypt, (2020).
[10] H.T. Nguyen, J.M. Pearce, Automated quantification of solar photovoltaic potential in cities Overview: a new method to determine a city's solar electric potential by analysis of a distribution feeder given the solar exposure and orientation of rooftops, Int. Rev. Spatial Plan. Sustain. Develop. 1 (1) (2013) 49–60.

[11] Q. Yin, A. Li, C. Han, The role of solar photovoltaic roofs in energy-saving buildings: research progress and future development trends, Buildings 14 (10) (2024) 2075–5309.
[12] J. Schardt, H. te Heesen, Performance of roof-top PV systems in selected European countries from 2012 to 2019, Solar Energy 217 (2021) 235–244, https://doi.org/10.1016/j.solener.2021.02.001.
[13] D. Pan, Y. Bai, M. Chang, X. Wang, W. Wang, The technical and economic potential of urban rooftop photovoltaic systems for power generation in Guangzhou, China, Energy Build 277 (2022) 112591, https://doi.org/10.1016/j.enbuild.2022.112591.
[14] E. Fakhraian, M. Alier, F. Valls Dalmau, A. Nameni, M.J. Casañ Guerrero, The urban rooftop photovoltaic potential determination, Sustainability 13 (13) (2021) 7447.
[15] A. Gomez-Exposito, A. Arcos-Vargas, F. Gutierrez-Garcia, On the potential contribution of rooftop PV to a sustainable electricity mix: the case of Spain, Renew. Sustain. Energy Rev. 132 (2020) 110074, https://doi.org/10.1016/j.rser.2020.110074.
[16] T. Hong, M. Lee, C. Koo, K. Jeong, J. Kim, Development of a method for estimating the rooftop solar photovoltaic (PV) potential by analyzing the available rooftop area using Hillshade analysis, Appl. Energy 194 (2017) 320–332, https://doi.org/10.1016/j.apenergy.2016.07.001.
[17] A. Walch, R. Castello, N. Mohajeri, J.-L. Scartezzini, Big data mining for the estimation of hourly rooftop photovoltaic potential and its uncertainty, Appl. Energy 262 (2020) 114404, https://doi.org/10.1016/j.apenergy.2019.114404.
[18] H. Alhammami, H. An, Techno-economic analysis and policy implications for promoting residential rooftop solar photovoltaics in Abu Dhabi, UAE, Renew. Energy 167 (2021) 359–368, https://doi.org/10.1016/j.renene.2020.11.091.
[19] R. Zhu, et al., The effect of urban morphology on the solar capacity of three-dimensional cities, Renew. Energy 153 (2020) 1111–1126, https://doi.org/10.1016/j.renene.2020.02.050.
[20] D. Li, X. Cui, L. Shi, Y. Li, An overview of the research on the correlation between solar energy utilization potential and spatial morphology, Results Eng. 24 (2024) 103444, https://doi.org/10.1016/j.rineng.2024.103444.
[21] Z. Ren, Y. Chen, C. Song, M. Liu, A. Xu, Q. Zhang, Economic analysis of rooftop photovoltaics system under different shadowing conditions for 20 cities in China, Build Simul. 17 (2) (2024) 235–252, https://doi.org/10.1007/s12273-023-1082-5.
[22] M. Xie, et al., The impact of urban morphology on the building energy consumption and solar energy generation potential of university dormitory blocks, Sustain. Cities Soc. 96 (2023) 104644, https://doi.org/10.1016/j.scs.2023.104644.
[23] P. Wang, Z. Liu, L. Zhang, Sustainability of compact cities: a review of inter-building effect on building energy and solar energy use, Sustain. Cities Soc. 72 (2021) 103035, https://doi.org/10.1016/j.scs.2021.103035.
[24] J. Li, Y. Wang, Y. Xia, A novel geometric parameter to evaluate the effects of block form on solar radiation towards sustainable urban design, Sustain. Cities Soc. 84 (2022) 104001, https://doi.org/10.1016/j.scs.2022.104001.
[25] J. Liu, C. Peng, J. Zhang, Understanding the relationship between rural morphology and photovoltaic (PV) potential in traditional and non-traditional building clusters using shapley additive exPlanations (SHAP) values, Appl. Energy 380 (2025) 125091, https://doi.org/10.1016/j.apenergy.2024.125091.
[26] R. Mahmoud, J.M. Kamara, N. Burford, Opportunities and limitations of building energy performance simulation tools in the early stages of building design in the UK, Sustainability 12 (22) (2020) 9702.
[27] Z. Jiang, et al., Physics-informed machine learning for building performance simulation-a review of a nascent field, Adv. Appl. Energy 18 (2025) 100223, https://doi.org/10.1016/j.adapen.2025.100223.
[28] A. El Abagy, M. Emeara, A. AbdelGawad, Orientation-optimization simulation for solar photovoltaic plant of Cairo international airport, Egypt. Int. J. Eng. Sci. Technol., 33(Mechanical Engineering) (2021) 45–68.
[29] M. Elkelawy, A.E. Mohamed, H.E. Seleem, Optimizing photovoltaic power plant efficiency: a comprehensive study on design, implementation, and sustainability, Pharos Eng. Sci. J. 2 (1) (2025) 12–22.
[30] A.A. Hassan, D.M. Atia, H.T. El-Madany, A.Y. Eliwa, Performance assessment of a 30.26 kW grid-connected photovoltaic plant in Egypt, Clean Energy 8 (6) (2024) 120–133.
[31] B. Ghaleb, M. Asif, Application of solar PV in commercial buildings: Utilizability of rooftops, Energy Build 257 (2022) 111774, https://doi.org/10.1016/j.enbuild.2021.111774.
[32] S. Izquierdo, M. Rodrigues, N. Fueyo, A method for estimating the geographical distribution of the available roof surface area for large-scale photovoltaic energy-potential evaluations, Solar Energy 82 (10) (2008) 929–939, https://doi.org/10.1016/j.solener.2008.03.007.
[33] L. Taggart, BR209: site layout planning for daylight and sunlight: a guide to good practice, 2022—a review, J. Building Survey, Appraisal Valuation 11 (4) (2023) 355–363.
[34] M.E. Fernández, J.O. Gentili, A.M. Campo, Solar access: review of the effective legal framework for an average argentine city, Renew. Sustain. Energy Rev. 156 (2022) 112008, https://doi.org/10.1016/j.rser.2021.112008.
[35] A.V. Tatachar, Comparative assessment of regression models based on model evaluation metrics, Int. Res. J. Eng. Technol. (IRJET) 8 (09) (2021) 2356–2395.
[36] J.S. Long, L.H. Ervin, Using heteroscedasticity consistent standard errors in the linear regression model, Am. Stat. 54 (3) (2000) 217–224.
[37] G. James, D. Witten, T. Hastie, R. Tibshirani, An introduction to statistical learning: with applications in R, Springer, 2013.
[38] M.H. Kutner, C.J. Nachtsheim, J. Neter, W. Li, Applied linear statistical models, 5th Edition. in McGrwa-Hill international edition. McGraw-Hill Irwin, (2005). [Online]. Available: https://books.google.co.uk/books?id=0xqCAAAACAAJ.
[39] S. Edalati, M. Ameri, M. Iranmanesh, Comparative performance investigation of mono- and poly-crystalline silicon photovoltaic modules for use in grid-connected photovoltaic systems in dry climates, Appl. Energy 160 (2015) 255–265, https://doi.org/10.1016/j.apenergy.2015.09.064.
[40] M.C. Alibuhtto, T.S.G. Peiris, Principal component regression for solving multicollinearity problem, 5 th International Symposium 2015 – IntSym (2015), SEUSL, 2015, Accessed: Sep. 27, 2025. [Online]. Available: http://ir.lib.seu.ac.lk/handle/123456789/1297.